Precipitation Structure and Processes of Typhoon Nari (2001): A Modeling Propsective

Ming-Jen Yang
Institute of Hydrological Sciences, National Central University

1. Introduction

Typhoon Nari (2001) struck Taiwan on 16 September 2001; it brought heavy rainfall, fresh flood, and caused severe economical and societal damage, including 92 human lives. The record-breaking 24-48 hour accumulated rainfall in many parts of Taiwan caused widespread flooding, and a great loss of human life and property damage. During the formation stage, Nari mostly stayed over the eastern Pacific Ocean with warm sea surface temperature above 29^{o}C. Both the air-sea interaction and large-scale atmospheric circulation contributed to the unique movement of Nari. Analysis revealed that Nari's heavy rains were due to warm ocean temperature, Nari's unique track and slow moving speed, and the steep terrain of Taiwan (Sui et al. 2002). The objective of this study is to investigate the key microphysical and precipitation processes responsible for heavy rainfalls of Typhoon Nari (2001).

2. Methodology

The NCAR-PSU MM5 model (Grell et al. 1995) version 3.5 is used to investigate the precipitation structure and processes associated with Typhoon Nari (2001). The MM5 model configuration includes 4 nested grids with horizontal resolutions of 60 km, 20 km, 6.67 km, and 2.22 km, respectively (Fig. 1); there are 31 sigma levels in the vertical. The simulation is integrated for 102 h, starting from 1800 UTC 15 September 2001. The initial and boundary conditions are taken from the ECMWF advanced global analysis with 1.25^{o} x 1.25^{o} horizontal resolution. Sea surface temperature is kept constant during the period of integration. The MM5 simulation uses the following physics options: 1) the Grell (1993) cumulus parameterization scheme, 2) the Reisner microphysics scheme with graupel (Reisner et al. 1998), 3) the MRF PBL scheme (Hong and Pan 1996), and 4) the atmospheric radiation scheme of Dudhia (1989). Note that no cumulus parameterization scheme is used on the 6.67-km and 2.22-km grids.

Because the vortex contained in the large-scale analysis is usually too weak and too broad, some method of typhoon initialization (or tropical cyclone bogussing) is required in order to improve the track and intensity forecast. We follows the method of Low-Nam and Davis (2001) to perform typhoon initialization. First the erroneously large vortex in the large-scale analysis is removed. Then an axis-symmetric Rankine vortex is inserted into the wind field, with the storm characteristics estimated from the JTWC best-track analysis. When constructing the three-dimensional bogus wind, the axis-symmetric wind is vertically weighted. The vertical weighting function is specified to be unity from the surface through 850 hPa, 0.95 at 700 hPa, 0.9 at 500 hPa, 0.7 at 300 hPa, 0.6 at 200 hPa and 0.1 at 100 hPa. Then the nonlinear balance equation is used to solve the corresponding geopotential height perturbation, and the hydrostatic equation is used to obtain the temperature perturbation. Moisture is assumed to be near saturated within the typhoon vortex.

3. Results

Figure 2 shows the MM5-simulated track (gray dot) of Typhoon Nari with topical cylone (TC) bogussing. The observed track (black dot) is also indicated for comparison. Without TC bogussing (not shown), the typhoon vortex was too weak; the typhoon center turned back once it hit the Central Mountain Range, and the typhoon track jumped around. On the other hand, with the TC bogussing (Fig. 2), the simulated vortex obtained the right intensity and structure similar to the observations, and the simulated typhoon track followed closely the observed track.

One of the reasons for Typhoon Nari to cause such a severe damage is its record-breaking 24-48 hour cumulated rainfall in many parts of Taiwan; therefore, it is interesting to examine the ability of the MM5 to predict the detailed precipitation distribution and amount. The observed and simulated 24-h rainfalls during the initial landfall stage (0000 LST 16 September to 0000 LST 17 September) of Typhoon Nari are shown in Fig. 3. This is the period when Nari’s rains overwhelmed existing flood protection capacities downstream of the Chi-Lung River in a part of Taipei that had no regulatory reservoirs, resulting in major flooding in the northern Taiwan (Sui et al. 2002). Basically the precipitation distribution was well simulated by the MM5, although the

simulated rainfall maximum (613.7 mm) was slightly more than the observed magnitude (437.6 mm).

One issue planned to explore in this study is the interaction between the microphysics and topographic processes for Typhoon Nari. In other words, how does the Central Mountain Range enhance or suppress the microphysical processes associated with Typhoon Nari? How does the Taiwan terrain modulate Nari's precipitation structure? Therefore, two vertical cross sections highlighting Nari's vertical precipitation structures are shown in Fig. 4. In particular, Cross Section AB shows Nari's vertical precipitation structure over the open ocean, and Cross Section CD shows Nari's vertical precipitation structure modified by the Taiwan terrain (Snow Mountain Range). Detailed model terrain on the 2.22-km grid is also displayed.

Figure 5 illustrates the simulated radar reflectivity and condensational heating fields at 0300 UTC 16 September 2001, 12 hours before the simulated Typhoon Nari makes landfall over the Keelung City. It clearly shows a symmetric structure with a typhoon eye, eyewall, and rainbands over the ocean. Large condensation heating associated with vertically upright convection mostly occurs in the middle to upper levels in the eyewall region, and the simulated Nari's eye has a horizontal scale of 40-50 km. On the other hand, when the simulated Typhoon Nari makes landfall at 1500 UTC 16 September (Fig. 6), Nari displays an evidently asymmetric structure due to the influence of Taiwan terrain. Condensational heating shows a vertically tilted structure over the mountain area, but the heating and convection over the ocean still display vertically upright orientation. Maximum heating of condensation heating occurs in the mid-to-upper level over the ocean, but the maximum heating locates in the low-to-middle level over the terrain area. Similar results are found in Wu et al. (2002) for Typhoon Herb (1996) case.

Several numerical experiments are planned to conduct in the near future to examine the sensitivity of simulated typhoon intensity, detailed precipitation structure, and rainfall amount to the choice and details of microphysics parameterization used in the model. Preliminary analysis suggested that the heavy rains in Nari (2001) contained many small raindrops (Sui et al. 2002); however, the heavy rains in Herb (1996), which also caused severe damage, contained more big raindrops. Three different microphysics parameterization schemes are planned to examine, including the warm-rain-only

microphysics scheme, a mixed-phase two-ice microphysics scheme (cloud ice and snow), and a three-ice microphysics scheme including graupel (cloud ice-snow-graupel). Wang (2002) showed in his idealized tropical-cyclone simulation that cloud structures of the simulated tropical cyclone could be quite different with various microphysics schemes. This study would like to extend Wang's idealized work to a real case, namely, the landfalling Typhoon Nari (2001). Another issue planned to explore is the interaction between the microphysics and topographic processes. In other words, how does the Taiwan terrain modulate Nari's precipitation structure? These issues are our future research directions in this modeling study of Typhoon Nari.

Reference

Davis, C. A., and S. Low-Nam, 2001: The NCAR-AFWA tropical cyclone bogussing scheme. A report prepared for the Air Force Weather Agency (AFWA). 12 pp. (Available from http://www.mmm.ucar.edu/mm5/mm5v3/tc-report.pdf)

Dudhia, J. 1989: Numerical simulation of convection observed during the Winter Monsoon Experiment using a mesoscale two-dimensional model. *J. Atmos. Sci*., **46**, 3077-3107.

Grell, G. A., 1993: Prognostic evaluation of assumptions used by cumulus parameterizations. *Mon. Wea. Rev*., **121**, 764-787.

Grell, G. A., J. Dudhia, and D.R.Stauffer,1995: A description of the fifth-generation Penn State/NCAR Mesoscale Model. NCAR Technical Note,122 pp.

Hong, S.-Y., and H.-L. Pan, 1996: Nocturnal boundary layer vertical diffusion in a medium-range forecast model. *Mon. Wea. Rev.*, **124**, 2322-2339.

Low-Nam, S., and C. Davis, 2001: Development of a tropical cyclone bogussing scheme for the MM5 system. Preprint, *The 11th PSU-NCAR MM5 Users' Workshop*, 130-134.

Reisner, J., R. J. Rasmussen, and R. T. Bruitjes, 1998: Explicit forecasting of supercooled liquid water in winter storms using the MM5 mesoscaled model. *Quart. J. Roy. Meteor. Soc*., **124**, 1071-1107.

Sui, C.-H., and Coauthors, 2002: Meteorology-hydrology study targets Typhoon Nari and Taipei flood.. *Eos*, Transctions, AGU, **83**, 265, 268-270.

Wang, Y., 2002: An explicit simulation of tropical cyclones with a triply nested movable mesh primitive equation model: TCM3. Part II: Model refinements and sensitivity to cloud microphysics parameterization. *Mon. Wea. Rev.*, **130**, 3022-3036.

Wu, C.-C., T.-H. Yen, Y.-H. Kuo, and W. Wang, 2002: Rainfall simulation associated with Typhoon Herb (1996) near Taiwan. Part I: The topographic effect. *Wea. Forecasting,* **17**, 1001-1015.

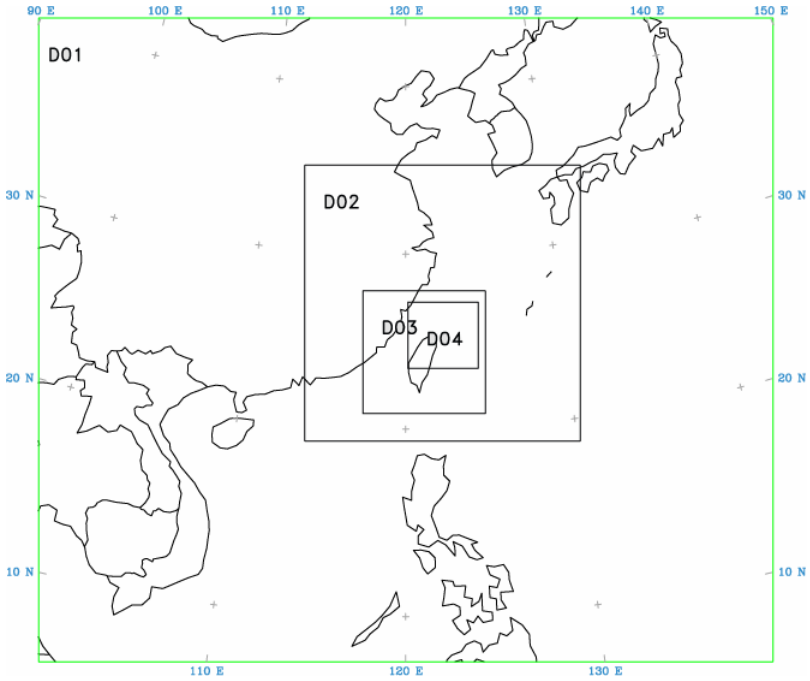

Fig. 1 Computational domains for four nested grids.

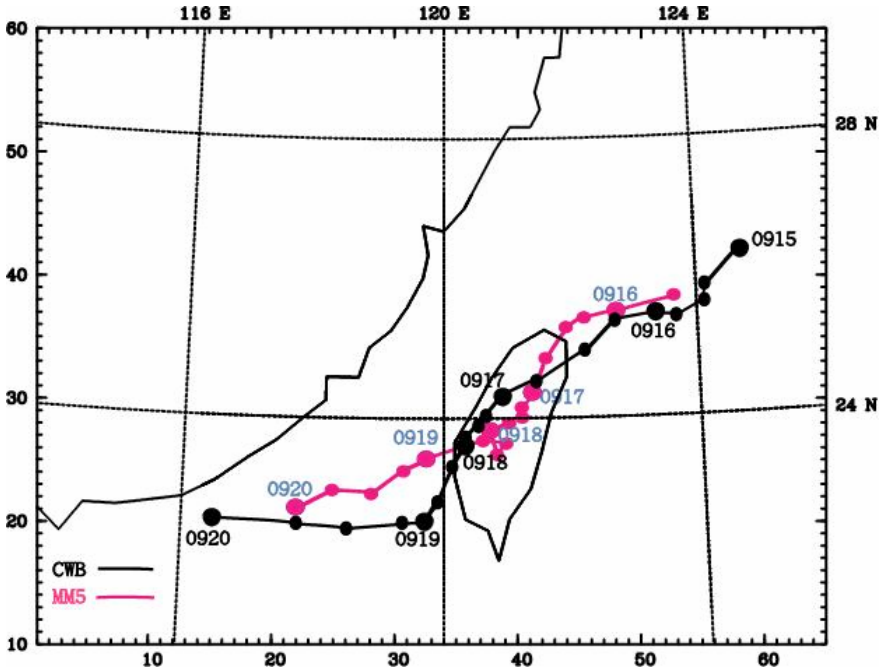

Fig.2. The tracks of Typhoon Nari. The black line is the best track provided by the Central Weather Bureau and the gray line is MM5-predicted track; a dot along the line represents the position of typhoon center every 6 h.

a) b)

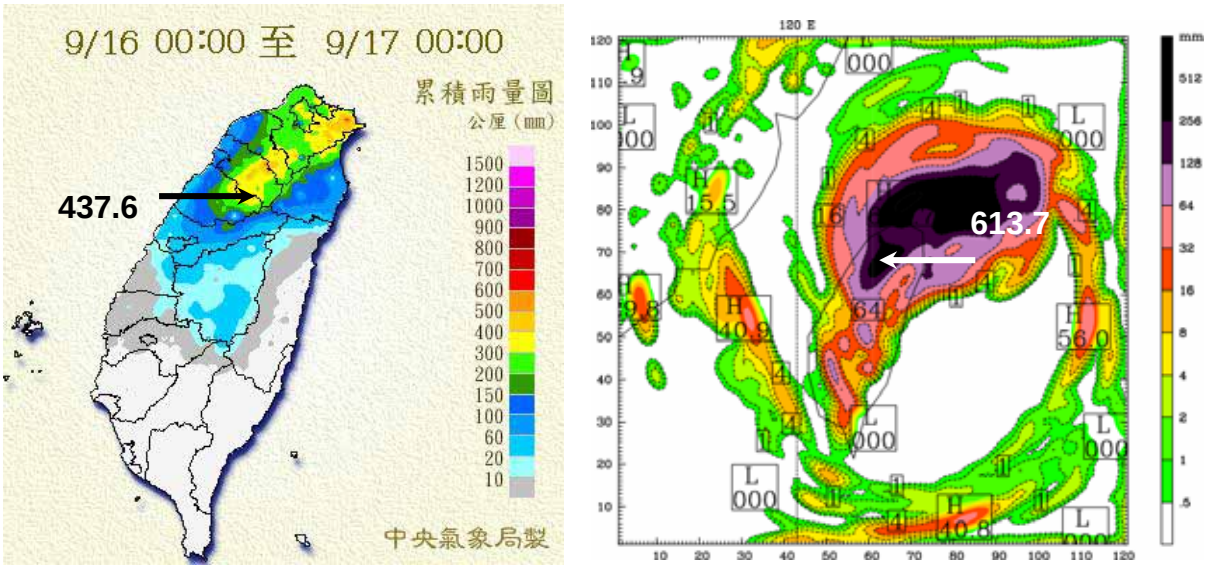

Fig. 3 (a) The observed 24-h rainfall (0000 LST 16 September to 0000 LST 17 September) and (b) the corresponding MM5 simulated 24-h rainfall (in units of mm) on 6.67-km grid.

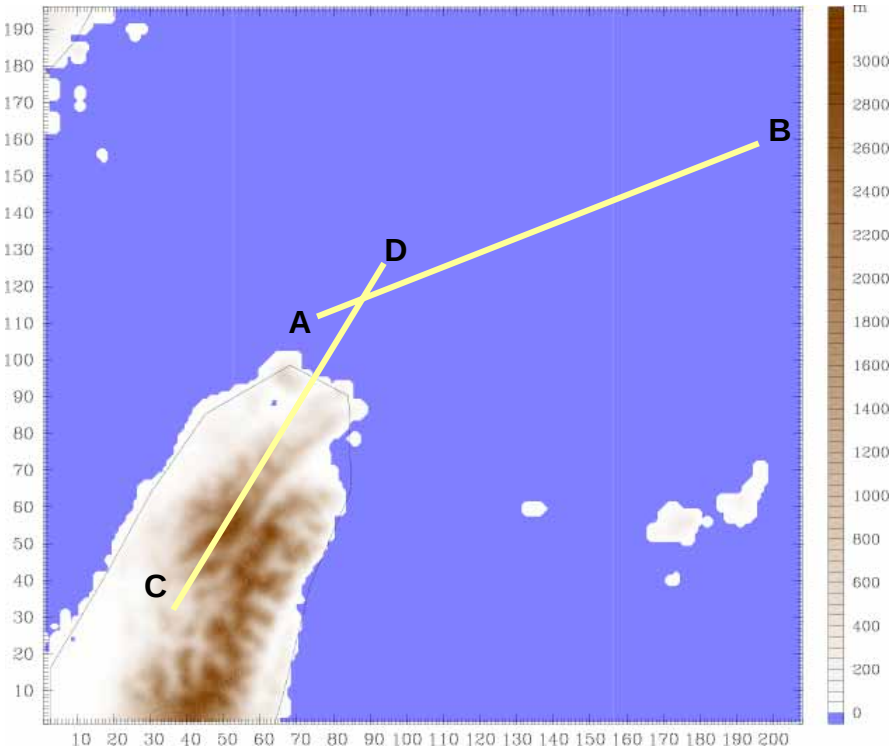

Fig. 4. The model terrain of domain 4 (2.22-km grid). Horizontal positions of vertical cross section AB and CD are indicated.

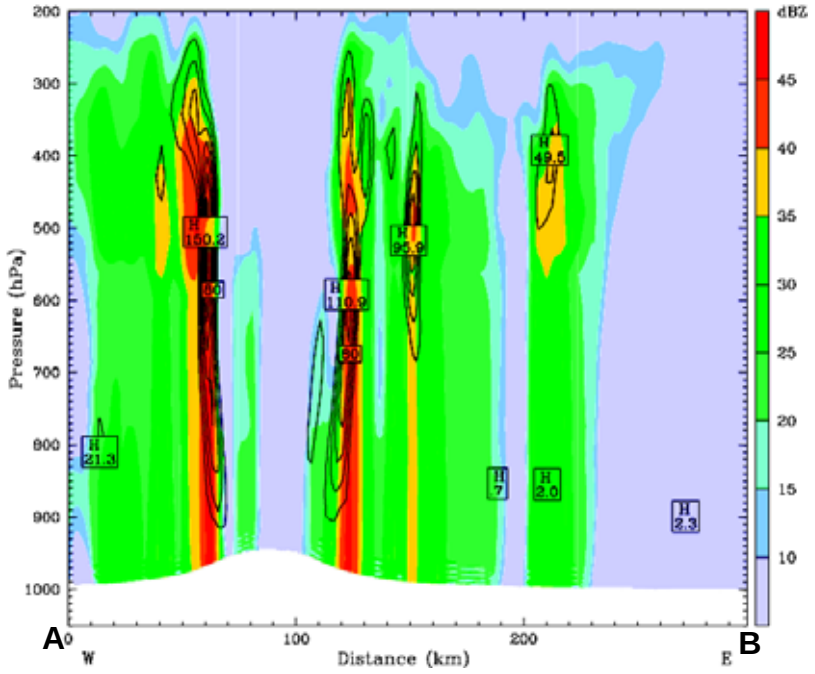

Fig. 5. Vertical cross section AB of simulated radar reflectivity (in units of dBZ; colored) and condensational heating (in units of Kh^{-1}; contoured) at 0300 UTC 16 September 2001.

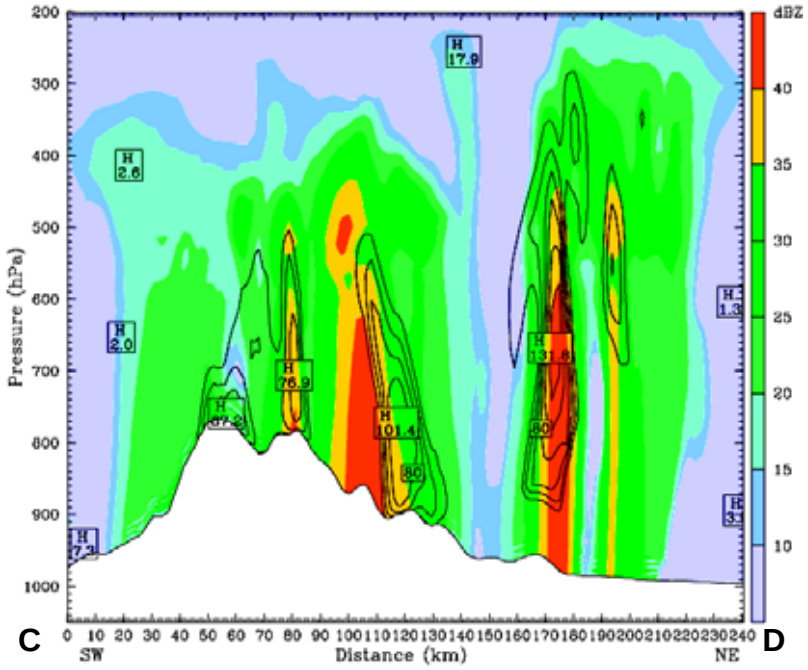

Fig. 6. Vertical cross section CD of simulated radar reflectivity (in units of dBZ; colored) and condensational heating (in units of Kh^{-1}; contoured) at 1500 UTC 16 September 2001.